

Artificial G-Wire Switch with 2,2'-Bipyridine Units Responsive to Divalent Metal Ions

Daisuke Miyoshi,[†] Hisae Karimata,^{†,‡} Zhong-Ming Wang,[†] Kazuya Koumoto,[†] and Naoki Sugimoto^{*,†,‡}

Contribution from the Frontier Institute for Biomolecular Engineering Research (FIBER), and Department of Chemistry, Faculty of Science and Engineering, Konan University, 8-9-1 Okamoto, Higashinada-ku, Kobe 658-8501, Japan

Received December 13, 2006; E-mail: sugimoto@konan-u.ac.jp

Abstract: Development of a guanine nanowire (G-wire) that is controllable and can be switched by external signals is important for the creation of molecular electronic technologies. Here, we constructed a G-wire in which the thymines of the main chain of d(G₄T₄G₄) were replaced with 2,2'-bipyridine units, which have two aromatic rings that rotate arbitrarily upon coordination with metal ions. Circular dichroism of the DNA oligonucleotides with or without the 2,2'-bipyridine unit showed that divalent metal ions induce the bipyridine-containing oligonucleotide to switch from an antiparallel to a parallel G-quadruplex. Native polyacrylamide gel electrophoresis showed that the parallel-stranded G-quadruplex DNA had a high-order structure. Circular dichroism and native gel electrophoresis analyses suggested that adding Na₂EDTA causes a reverse structural transition from a parallel-stranded high-order structure to an antiparallel G-quadruplex. Moreover, atomic force microscopy showed a long nanowire (~200 nm) in the presence of Ni²⁺ but no significant image in the absence of Ni²⁺ or in the presence of both Ni²⁺ and Na₂EDTA. These observations revealed that the parallel-stranded high-order structure is a G-wire containing numerous DNA oligonucleotide strands bound together via divalent metal ion–2,2'-bipyridine complexes. Finally, we found that alternating addition of Ni²⁺ and Na₂EDTA can cycle the G-wire between the high-order and disorganized structures, with an average cycling efficiency of 0.95 (i.e., 5% loss per cycle). These results demonstrate that a DNA oligonucleotide incorporating the 2,2'-bipyridine unit acts as a G-wire switch that can be controlled by chemical input signals, namely, divalent metal ions.

Introduction

Switchable and controllable nanodevices are necessary for generating nanomaterials whose structure and function can be dynamically regulated.^{1,2} DNA molecules offer substantial advantages for the design of such nanodevices because they have periodic one-, two-, and three-dimensional nanostructures.³ Almost all previous studies, however, have utilized sequence-specific duplexes to generate self-assembled DNA nanostructures. Moreover, although some of the DNA nanostructures based on DNA duplexes are switchable, controllable, and addressable, functionalizing them by template assemblies of

metal ions or with functional materials is time-consuming and laborious. Thus, DNA duplexes are not ideal for practical applications.

Guanine nanowires (G-wires) are an alternative functional DNA nanostructure. These are based on a four-stranded DNA helix called a G-quadruplex.⁴ The G-quadruplex is formed by guanine-rich DNA sequences such as telomere DNAs with cyclic Hoogsteen base pairs between four guanine bases in a coplanar arrangement.⁵ G-wire structures have been studied by many researchers because of their peculiar characteristics. For example, Chen reported that Sr²⁺ induces G-rich sequences such as d(G₄T₂G₄T₂G₄T₂G₄) and d(G₄T₄G₄T₄G₄T₄G₄) to form a G-wire structure.⁶ Using atomic force microscopy (AFM), Marsh et al. directly observed that d(G₄T₂G₄) forms a G-wire in the presence of Mg²⁺ and spermidine.^{4b} These authors also found that the G-wire is a one-dimensional nanowire with a uniform height and width and few bends or kinks.^{4b} We previously reported that Ca²⁺ and molecular crowding induces G-wire formation by telomere DNAs.⁷ Together, the results of these

[†] Frontier Institute for Biomolecular Engineering Research.

[‡] Department of Chemistry.

- (1) (a) Seeman, N. C. *Annu. Rev. Biophys. Biomol. Struct.* **1998**, *27*, 225–248. (b) Storhoff, J. J.; Mirkin, C. A. *Chem. Rev.* **1999**, *99*, 1849–1862. (c) Seeman, N. C. *Nature* **2003**, *421*, 427–431. (d) Gothelf, K. V.; LaBean, T. H. *Org. Biomol. Chem.* **2005**, *3*, 4023–4937.
- (2) (a) Mao, C.; Sun, W.; Shen, Z.; Seeman, N. C. *Nature* **1999**, *397*, 144–146. (b) Yurke, B.; Turberfield, A. J.; Mills, A. P., Jr.; Simmel, F. C.; Neumann, J. L. *Nature* **2000**, *406*, 605–608. (c) Yan, H.; Zhang, X.; Shen, Z.; Seeman, N. C. *Nature* **2002**, *415*, 62–65.
- (3) (a) Chen, J.; Seeman, N. C. *Nature* **1991**, *350*, 631–633. (b) Zhang, Y.; Seeman, N. C. *J. Am. Chem. Soc.* **1994**, *116*, 1661–1669. (c) Winfree, E.; Liu, F.; Wenzler, L. A.; Seeman, N. C. *Nature* **1998**, *394*, 539–544. (d) Mao, C.; Sun, W.; Seeman, N. C. *J. Am. Chem. Soc.* **1999**, *121*, 5437–5443. (e) LaBean, T. H.; Yan, H.; Kopatsch, J.; Liu, F.; Winfree, E.; Reif, J. H.; Seeman, N. C. *J. Am. Chem. Soc.* **2000**, *122*, 1848–1860. (f) Shih, W. M.; Quispe, J. D.; Joyce, G. F. *Nature* **2004**, *427*, 618–621. (g) Rothmund, P. W. K. *Nature* **2006**, *440*, 297–302.

- (4) (a) Marsh, T. C.; Henderson, E. *Biochemistry* **1994**, *33*, 10718–10724. (b) Marsh, T. C.; Vesenka, J.; Henderson, E. *Nucleic Acids Res.* **1995**, *23*, 696–700. (c) Davis, J. T. *Angew. Chem., Int. Ed.* **2004**, *43*, 668–698.
- (5) (a) Sen, D.; Gilbert, W. *Nature* **1988**, *334*, 364–366. (b) Blackburn, E. H. *Nature* **1991**, *350*, 569–573. (c) Keniry, M. A. *Biopolymers* **2001**, *56*, 123–1246.
- (6) Chen, F. M. *Biochemistry* **1992**, *31*, 3769–3776.

previous studies indicate that the one-dimensional G-wire can be used as a structurally well-defined nanoscaffold.

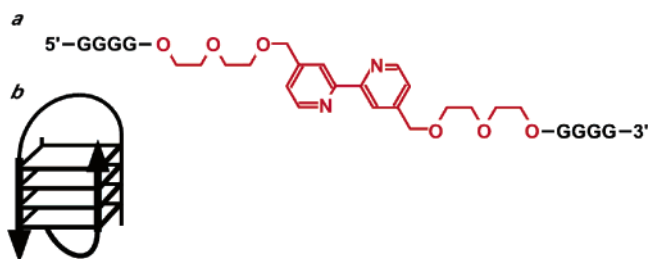
There is growing interest in guanine-rich sequences as functional elements in molecular electronics because guanine has the lowest oxidation potential of the deoxynucleotide bases.⁸ Theoretical studies have further suggested that the G-wire structure possesses enough conductivity for use in nanoscale biomolecular electronics.⁹ Thus, the G-wire structure possesses structural and electronic advantages as a nanomaterial; however, a means of controlling or switching G-wire formation has not yet been developed because the G-wire is an aggregated developed structure. Therefore, further studies are needed to develop a G-wire switch that can be controlled by chemical inputs.

Here, we designed and synthesized a DNA that can undergo a reversible structural transition between a compact antiparallel G-quadruplex and a long G-wire, depending on external signals. To enable a reversible structural transition, we replaced the thymines in the d(G₄T₄G₄) chain with a metal ion-responsive unit, 2,2'-bipyridine, which is composed of two aromatic rings that rotate arbitrarily upon coordination with metal ions.¹⁰ Structural analysis utilizing circular dichroism (CD) and native polyacrylamide gel electrophoresis (PAGE) showed that the DNA that included the 2,2'-bipyridine units underwent a structural transition from an antiparallel G-quadruplex to a high-order parallel-stranded G-quadruplex upon addition of divalent metal ions such as Ni²⁺, Co²⁺, and Zn²⁺. In addition, Na₂EDTA induced a reversible structural transition from the high-order structure to the antiparallel G-quadruplex. Moreover, direct observation of the reversible structural transition using AFM showed that the high-order parallel-stranded structure is a G-wire that contains numerous DNA oligonucleotides, which demonstrates that the G-wire can be switched by divalent metal ions and Na₂EDTA. Alternating addition of Ni²⁺ and Na₂EDTA showed that the G-wire could be switched up to 8 times, with a cycling efficiency of 0.95 (i.e., only 5% loss per cycle). These results demonstrated that the G-wire switch developed here can be readily controlled by chemical signals. Notably, in the presence of divalent metal ions, the G-wire switch forms an array of divalent metal ions because divalent metal ion–2,2'-bipyridine complexes are adjacent to each G-quadruplex unit and are separated by approximately 1.5 nm. This allows the conductivity of the G-wire to be increased and introduces addressability into the G-wire.

Results and Discussion

Design of Oligonucleotides that Can Switch from a G-Quadruplex to a G-Wire. DNA containing a main-chain modification with a linker that tightly binds metal ions has been shown to form a supramolecular structure.¹¹ In particular, 2,2'-bipyridine, which contains two pyridine rings that rotate arbitrarily upon coordination with metal ions, has been inserted into DNA to generate supramolecular structures and functional

Chart 1



systems because it strongly chelates metals, is stable to redox changes, and is easily added as a functional group.¹² Peptides containing 2,2'-bipyridine functionality spontaneously fold into coiled-coil α -helix or β -sheet structures in the presence of metal ions.¹³ Moreover, a nucleoside mimic in which the heterocyclic base is replaced by 2,2'-bipyridine undergoes metal-mediated base pair formation.¹⁴ Thus, 2,2'-bipyridine could be useful for controlling DNA structures. We replaced the main-chain thymines in d(G₄T₄G₄) with 2,2'-bipyridine, connected to the main chain via ether linkages (bipy), generating d(G₄-bipy-G₄) (G1; Chart 1a). We synthesized G1 using a bipy phosphoramidite (see the Supporting Information and ref 10) and d(G₄T₄G₄) (G2) as a control. Previous studies have shown that, in the presence of Na⁺, G2 forms a hairpin dimer antiparallel G-quadruplex with thymine residues in the loop (Chart 1b).¹⁵

Figure 1a shows CD spectra for 5 μ M G1 in the absence of divalent metal ions or the presence of 2.5 μ M Mg²⁺, Ca²⁺, Zn²⁺, Co²⁺, or Ni²⁺ in a buffer containing 100 mM NaCl and 50 mM MES (pH 6.0) at 4 °C. The CD spectra for G1 without divalent metal ions and in the presence of Ca²⁺ or Mg²⁺ show negative and positive peaks near 260 and 295 nm, respectively, indicating an antiparallel G-quadruplex.¹⁶ Surprisingly, the CD spectra for G1 in the presence of Zn²⁺, Co²⁺, or Ni²⁺ had positive and negative peaks near 260 and 240 nm, respectively, indicating that it forms a parallel-oriented G-quadruplex.¹⁷ These results show that these divalent metal ions induce a structural transition from an antiparallel to a parallel G-quadruplex. The CD spectra for G1 in the presence of Zn²⁺, Co²⁺, or Ni²⁺ had a small positive peak at 295 nm, indicating that the structural transition from the antiparallel G-quadruplex to the G-wire does not proceed perfectly, because the structural transition of G1 induced by the divalent metal ions may be in equilibrium.¹⁸ On the other hand, the CD spectra for G2 indicated an antiparallel G-quadruplex structure in the presence or absence of divalent metal

- (7) (a) Miyoshi, D.; Nakao, A.; Sugimoto, N. *Nucleic Acids Res.* **2003**, *31*, 1156–1163. (b) Miyoshi, D.; Karimata, H.; Sugimoto, N. *Angew. Chem., Int. Ed.* **2005**, *44*, 3740–3744.
- (8) (a) Bixon, M.; Giese, B.; Wessely, S.; Langenbacher, T.; Michel-Beyerle, M. E.; Jortner, J. *Proc. Natl. Acad. Sci. U.S.A.* **1999**, *96*, 11713–11716. (b) Porath, D.; Bezryadin, A.; de Vries, S.; Dekker, C. *Nature* **2000**, *403*, 635–638.
- (9) Calzolari, A.; Felice, R. D.; Molinari, E.; Garbesi, A. *Appl. Phys. Lett.* **2002**, *80*, 3331–3333.
- (10) Wiederholt, K.; McLaughlin, L. W. *Nucleic Acids Res.* **1999**, *27*, 2487–2493.

- (11) (a) Stewart, K. M.; McLaughlin, L. W. *J. Am. Chem. Soc.* **2004**, *126*, 2050–2057. (b) Mitra, D.; Di Cesare, N.; Sleiman, H. F. *Angew. Chem., Int. Ed.* **2004**, *43*, 5804–5808. (c) Stewart, K. M.; Rojo, L.; McLaughlin, L. M. *Angew. Chem., Int. Ed.* **2004**, *43*, 5808–5811. (d) Choi, J. S.; Kang, C. W.; Jung, K.; Yang, J. W.; Kim, Y. G.; Han, H. *J. Am. Chem. Soc.* **2004**, *126*, 8606–8607.
- (12) (a) Fujita, M.; Kwon, Y. J.; Washizu, S.; Ogura, K. *J. Am. Chem. Soc.* **1994**, *116*, 1151–1152. (b) Kaes, C.; Katz, A.; Hosseini, M. W. *Chem. Rev.* **2000**, *100*, 3553–3590.
- (13) (a) Ghadiri, M. R.; Soares, C.; Choi, C. *J. Am. Chem. Soc.* **1992**, *114*, 825–831. (b) Schneider, J. P.; Kelly, J. W. *J. Am. Chem. Soc.* **1995**, *117*, 2533–2546.
- (14) Weizman, H.; Tor, Y. *J. Am. Chem. Soc.* **2001**, *123*, 3375–3376.
- (15) Schultze, P.; Smith, F. W.; Feigon, J. *Structure* **1994**, *2*, 221–233.
- (16) Balagurumoorthy, P.; Brahmachari, S. K. *J. Biol. Chem.* **1994**, *269*, 21858–21869.
- (17) (a) Lu, M.; Guo, Q.; Kallenbach, N. R. *Biochemistry* **1993**, *32*, 598–601. (b) Wyatt, J. R.; Davis, P. W.; Freier, S. M. *Biochemistry* **1996**, *35*, 8002–8008. (c) Miyoshi, D.; Nakao, A.; Toda, T.; Sugimoto, N. *FEBS Lett.* **2001**, *496*, 128–133.
- (18) We investigated the structure of G1 in the presence of higher concentrations of Ni²⁺. However, much higher concentrations of Ni²⁺, for example, 1 mM, led to the aggregation and precipitation of G1.

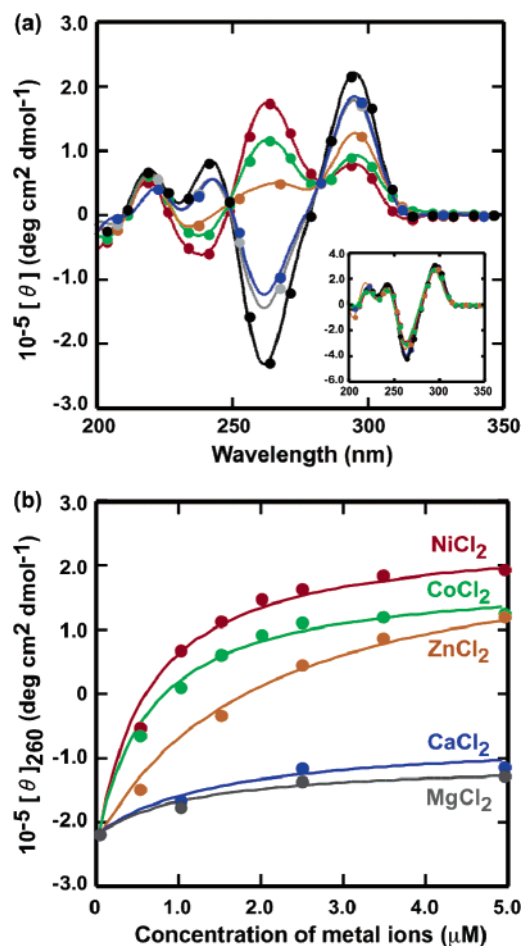


Figure 1. (a) CD spectra for 5 μM G1 in a buffer containing 100 mM NaCl and 50 mM MES (pH 6.0) in the absence of divalent metal ions (black) or presence of 2.5 μM MgCl_2 (gray), CaCl_2 (blue), ZnCl_2 (orange), CoCl_2 (light green), or NiCl_2 (red) at 4 $^\circ\text{C}$. Inset: CD spectra for 5 μM G2 under the same conditions. (b) CD intensity changes at 260 nm for 5 μM G1 in a buffer containing 100 mM NaCl, 50 mM MES (pH 6.0), and various concentrations of MgCl_2 (gray), CaCl_2 (blue), ZnCl_2 (orange), CoCl_2 (light green), or NiCl_2 (red) at 4 $^\circ\text{C}$.

ions (Figure 1a, inset). These results suggest that interactions between divalent metal ions and the bipy units cause G1 to form parallel-oriented G-quadruplexes.

We further investigated the structure of G1 in the presence of K^+ because a coexisting monovalent cation is critical for the structure and stability of G-quadruplexes. CD spectra for 5 μM G1 in a buffer containing 100 mM KCl and 50 mM MES (pH 6.0) at 4 $^\circ\text{C}$ had two positive peaks at around 260 and 295 nm (Supporting Information Figure S1), indicating a mixture of parallel and antiparallel G-quadruplexes or a mixed chair-type G-quadruplex, which has been observed in human telomere sequences in the presence of K^+ .¹⁹ Although the CD spectra for G1 in the presence of K^+ showed that Ni^{2+} can induce the antiparallel–parallel structural transition as seen in the presence of Na^+ , the structure of G1 in the absence of Ni^{2+} remains unclear. Therefore, Na^+ may be a more suitable coexisting monovalent cation for constructing a DNA structural switch than K^+ .

Figure 1b shows the change in CD intensity at 260 nm, where the antiparallel and parallel G-quadruplexes have negative and

positive peaks, respectively, for 5 μM G1 in buffers containing 100 mM NaCl, 50 mM MES (pH 6.0), and various concentrations of divalent metal ions at 4 $^\circ\text{C}$. The changes in CD intensity clearly indicated that a structural transition from an antiparallel to a parallel G-quadruplex was induced by adding Zn^{2+} , Co^{2+} , or Ni^{2+} but not Ca^{2+} or Mg^{2+} . To estimate the apparent binding constant for divalent metal ions from the titration curves, the CD intensity changes for G1 at 260 nm were fitted to the following equation:²⁰ $\text{CD intensity at 260 nm} = a[\text{M}^{2+}]/([\text{M}^{2+}] + 1/K_a) + b$, where a is the scale factor, b is the initial CD value, and K_a is the apparent binding constant for divalent metal ions.

The free energy change (ΔG°) for the formation of the divalent metal ion–G1 complexes was calculated as $\Delta G^\circ = -RT \ln K_a$, where R and T are the gas constant and temperature (K), respectively. The ΔG° values at 4 $^\circ\text{C}$ for the formation of the Ni^{2+} –G1, Co^{2+} –G1, and Zn^{2+} –G1 complexes were estimated to be -7.8 , -7.7 , and -7.2 kcal mol⁻¹, respectively. The order of stability of the G1–divalent metal ion complexes was consistent with that of the stability of coordination between the bipy and divalent metal ions (Supporting Information Figure S2).²¹ Although the differences between these ΔG° values are not significant, these results imply that interaction between the divalent metal ions and bipy units is essential for the structural transition of G1. These results are also consistent with the conclusions drawn on the basis of the CD spectra for G1 and G2 (Figure 1a), which indicated that the bipy unit is required for the transition. Notably, only 2 μM Ni^{2+} was sufficient for the structural transition. In contrast, 1 mM Sr^{2+} or 20 mM Ca^{2+} have been reported to facilitate G-wire formation by natural telomeric sequences.^{6,7a} In addition, Ni^{2+} in the concentration range of several mM can induce G-wire formation of G2 (data not shown). In comparison with the natural G-quadruplexes, G1 requires a concentration of divalent metal ions that is 3–4 orders of magnitude lower to undergo the structural transition. This lower concentration of divalent metal ions should greatly enhance the reversibility of the structural switch because waste products, such as excess divalent metal ions, can reduce the switching efficiency.

Structural Transition of G1 Induced by Divalent Metal Ions. Because CD spectra alone are not sufficient for demonstrating G-quadruplex structures,⁷ we confirmed the structural transition of 5 μM G1 by native PAGE in the presence of 2.5 μM divalent metal ions (Figure 2). The bands for G1 became smeared and migrated more slowly in the presence of Zn^{2+} , Co^{2+} , or Ni^{2+} but not in the presence of Ca^{2+} or Mg^{2+} . The presence of slower, smeared bands indicated that G1 included heterogeneous and high-order structures such as G-wires composed of multiple parallel-oriented strands. In addition, G1 in the presence of Zn^{2+} or Co^{2+} showed two main bands, which may correspond to tetramers and octamers of G1. These results are consistent with the CD spectra because the G-wire formation as well as the tetramer and octamer formations require a parallel strand orientation.^{4a,b} It is noteworthy that the main bands

(19) (a) Zhang, N.; Phan, A. T.; Patel, D. J. *J. Am. Chem. Soc.* **2005**, *127*, 17277–17285. (b) Xu, Y.; Noguchi, Y.; Sugiyama, H. *Bioorg. Med. Chem.* **2006**, *15*, 5584–5591.

(20) Yamauchi, T.; Miyoshi, D.; Kubodera, T.; Nishimura, A.; Nakai, S.; Sugimoto, N. *FEBS Lett.* **2005**, *579*, 2583–2588. Note that the apparent binding constant just corresponds to the midpoint of the transition.

(21) Martell, E.; Smith, R. M. *Critical Stability Constants*, 1st Supplement; Plenum Press: New York and London, 1982; Vol. 5, p 248. Note that since free energy change was estimated with the apparent binding constant, this free energy change includes not only the divalent metal ion binding to G1 but also other factors such as structural transition of G1.

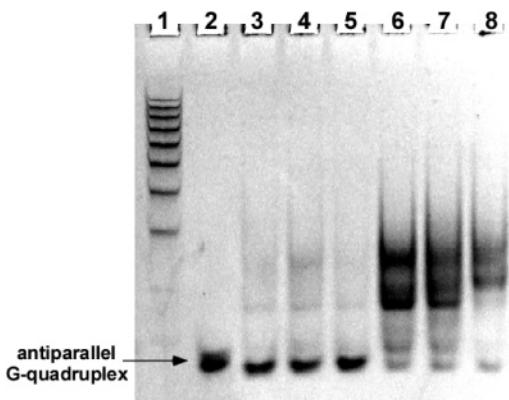


Figure 2. Native PAGE of 5 μM G1 in a buffer containing 100 mM NaCl and 50 mM MES (pH 6.0) in the absence or presence of 2.5 μM divalent metal ions at 4 $^{\circ}\text{C}$. Lane 1: 10 base pair DNA ladder as a size marker. Lane 2: G2 in the absence of metal ions as a marker for the antiparallel G-quadruplex. Lanes 3–8: G1 in the absence of metal ions (lane 3) and in the presence of MgCl_2 (lane 4), CaCl_2 (lane 5), ZnCl_2 (lane 6), CoCl_2 (lane 7), or NiCl_2 (lane 8).

observed in the presence of Zn^{2+} or Co^{2+} disappeared in the presence of Ni^{2+} . However, G1 migrating to the top of the gel was observed in the presence of Ni^{2+} . These observations suggest that G1 folds into higher-order structures in the presence of Ni^{2+} than in the presence of Zn^{2+} or Co^{2+} . These results are consistent with the CD spectra showing that the order of ability of divalent metal ions to induce the G-wire formation is $\text{Ni}^{2+} > \text{Co}^{2+} > \text{Zn}^{2+}$.

To investigate the mechanism of the structural transition of G1 from an antiparallel G-quadruplex to a G-wire, divalent metal ion binding to the 2,2'-bipyridine units was monitored by UV spectroscopy. Figure 3a shows the UV spectra for 20 μM G1 in buffers containing 100 mM NaCl, 50 mM MES (pH 6.0), and various concentrations of Ni^{2+} at 4 $^{\circ}\text{C}$. The UV spectrum for G1 in the absence of Ni^{2+} had a small shoulder at around 285 nm, which is characteristic of the bipyridine $\pi-\pi^*$ transition.^{14,22} Upon addition of Ni^{2+} , the shoulder decreased and a new shoulder was observed. Because G1 absorbs strongly at around 260 nm, a second band for the bipyridine $\pi-\pi^*$ transition normally found near 240 nm could not be observed. These changes in the spectra upon titration with Ni^{2+} can be observed more clearly in the UV differential spectra (Supporting Information Figure S3), which were obtained by subtraction of the UV spectrum for G1 in the absence of Ni^{2+} from that in the presence of Ni^{2+} . The UV differential spectra showed that there was a decrease in absorption at around 285 nm, which corresponds to the free 2,2'-bipyridine units, and an increase in absorption at around 307 nm, which is characteristic of the 2,2'-bipyridine–divalent metal ion complexes. Moreover, a plot of absorbance at 307 nm against the ratio of Ni^{2+} to G1, as shown in the inset of Figure 3a, suggested two important points: the titration curve is saturated with 20 μM G1, indicating that the dissociation constant of the formation of the G1 and Ni^{2+} complex is much smaller than 20 μM . This agrees with the CD titration curve shown in Figure 1b. The ratio of Ni^{2+} to G1 in formation of the complex is 1:3, which is consistent with the coordination number of Ni^{2+} . On the other hand, Ni^{2+} did not cause a change in the UV spectrum for G2 (Figure 3b). These

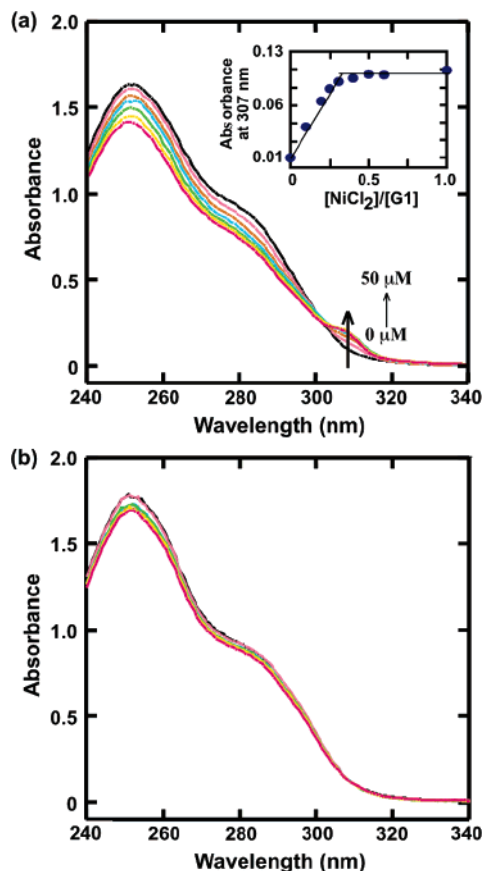


Figure 3. (a) UV absorption spectra for 20 μM G1 in a buffer containing 100 mM NaCl and 50 mM MES (pH 6.0), 100 mM NaCl, 50 mM MES (pH 6.0), and the following: 0 μM (black), 2 μM (pink), 4 μM (orange), 6 μM (light blue), 10 μM (yellow), 20 μM (light green), and 50 μM (red) NiCl_2 at 4 $^{\circ}\text{C}$. Inset: Plot of UV absorbance changes at 307 nm against the ratio of NiCl_2 to G1. (b) UV absorption spectra for 20 μM G2 in a buffer containing 100 mM NaCl and 50 mM MES (pH 6.0), 100 mM NaCl, 50 mM MES (pH 6.0), and the following: 0 μM (black), 2 μM (pink), 4 μM (orange), 6 μM (light blue), 10 μM (yellow), 20 μM (light green), and 50 μM (red) NiCl_2 at 4 $^{\circ}\text{C}$.

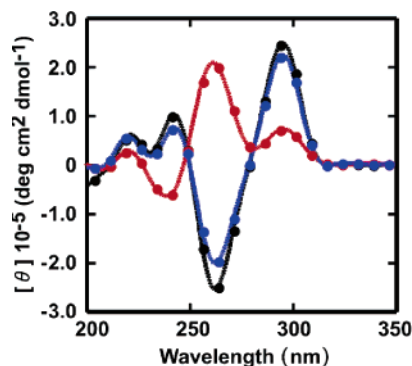


Figure 4. CD spectra for 5 μM G1 in buffers containing 100 mM NaCl, 50 mM MES (pH 6.0), and the following: no extra agent (black), 100 μM NiCl_2 (red), or 100 μM NiCl_2 plus 120 μM Na_2EDTA (blue) at 4 $^{\circ}\text{C}$.

results demonstrate that Ni^{2+} binds to 2,2'-bipyridine. On the basis of these results, it is reasonable to conclude that a divalent metal ion binding to the 2,2'-bipyridine induces a structural transition of G1 from an antiparallel G-quadruplex to a G-wire.

Reverse Structural Transition from a G-Wire to an Antiparallel G-Quadruplex. Next, we examined the reverse structural transition from a G-wire to an antiparallel G-

(22) (a) Weibel, N.; Charbonniere, L. J.; Guardigli, M.; Roda, A.; Ziessel, R. J. *Am. Chem. Soc.* **2004**, *126*, 4688–4896. (b) Sabbatini, N.; Guardigli, M.; Lehn, J. M. *Coord. Chem. Rev.* **1993**, *123*, 201–228.

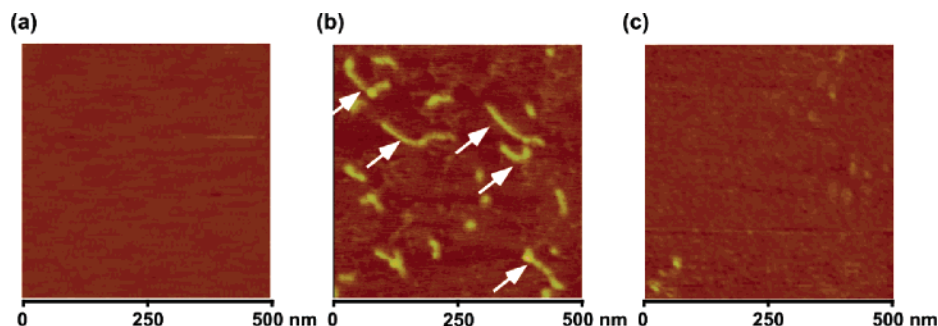


Figure 5. AFM images of the G-wire of G1 in buffers containing (a) 100 mM NaCl and 50 mM MES (pH 6.0) alone; (b) 100 mM NaCl, 50 mM MES (pH 6.0), and 50 μM NiCl_2 ; (c) 100 mM NaCl and 50 mM MES (pH 6.0), 50 μM NiCl_2 , and 100 μM Na_2EDTA . Images of the G-wire structures in panel b are indicated by arrows.

quadruplex. Figure 4 shows the CD spectra for 5 μM G1 in the absence of Ni^{2+} , the presence of 100 μM Ni^{2+} , and the presence of both 100 μM Ni^{2+} and 120 μM Na_2EDTA . The CD spectra in the absence and presence of Ni^{2+} show the formation of an antiparallel G-quadruplex and a G-wire, respectively, as observed in Figure 1a. On the other hand, the CD spectrum in the presence of both Ni^{2+} and Na_2EDTA shows positive and negative peaks at around 295 and 260 nm, respectively, indicating formation of an antiparallel G-quadruplex by G1. This indicates that Na_2EDTA can reverse the structural transition. It is noteworthy that the spectrum in the presence of both Ni^{2+} and Na_2EDTA is almost the same as that in the absence of Ni^{2+} , suggesting that the reverse structural transition induced by Na_2EDTA is very efficient. In addition, like Na_2EDTA , an immobilized chelator could induce the reverse structural transition from a G-wire to an antiparallel G-quadruplex (Supporting Information Figure S4), indicating that removal of the divalent metal ions from the bipy units is important for the reversible structural transition but that a direct interaction between the chelator and G1 is not.

The reverse structural transition was further verified by native PAGE. Figure S5 in the Supporting Information shows native PAGE of 5 μM G1 in the absence of Ni^{2+} , the presence of 100 μM Ni^{2+} , and the presence of both 100 μM Ni^{2+} and 120 μM Na_2EDTA . The migration of G1 in the presence of Ni^{2+} was typical of a G-wire as shown in previous studies^{4a,b,7} and in Figure 2 of the present study, whereas G1 formed a compact antiparallel G-quadruplex not only in the absence of Ni^{2+} but also in the presence of 100 μM Ni^{2+} and 120 μM Na_2EDTA . In addition, migration of G1 in the absence of Ni^{2+} and in the presence of Ni^{2+} and 120 μM Na_2EDTA was identical, indicating that the structures of G1 are very similar in these two conditions. The identical migration by G1 in the absence of Ni^{2+} and in the presence of Ni^{2+} and Na_2EDTA supports the idea that there is no direct interaction between Na_2EDTA and G1. These native PAGE results are consistent with the CD results (Figure 4) and with the finding that an immobilized chelator can induce the reverse structural transition (Supporting Information Figure S4). These results indicate that the reverse structural transition from a G-wire to an antiparallel G-quadruplex can be induced by Na_2EDTA and, therefore, that G1 can function as a G-wire switch controlled by Ni^{2+} and Na_2EDTA .

Direct Measurement of the Reversible Structural Transition. Structural analyses of G1 by CD and native PAGE indicated that G1 folded into a G-wire structure in the presence of Ni^{2+} . To further confirm these findings, we directly examined

the G-wire structure by AFM. Figure 5a shows a typical AFM image of G1 in the absence of Ni^{2+} . G1 was not visible, indicating that these conditions do not cause it to fold into a high-order structure that can be observed by AFM. In contrast, in the presence of Ni^{2+} , the AFM image revealed that G1 folded into a high-order linear structure (Figure 5b). Thus, AFM confirmed the findings from CD spectroscopy and native PAGE. In addition, static analyses indicated that the length of the G-wire ranged from several tens of nanometers to 200 nm, and that the average length of the G-wires (from 37 G-wire images) is 73 ± 40 nm. Although this is shorter than that reported previously for G-wires,^{4a} the average height of the G-wire observed in this study was 1.1 ± 0.3 nm (an average of 37 G-wire images), which is similar to that noted in a previous report.^{4a} Transmission electron microscopy (TEM) also demonstrated that G1 formed a wire up to 2 μm in length with few bends or branches in the presence of Ni^{2+} (Supporting Information Figure S6).

The characteristics of the mica surface for AFM measurements are very different from those of the carbon-coated grid used for TEM measurements. For example, the mica surface is hydrophilic, whereas the carbon-coated grid is hydrophobic. Thus, the difference in the observed lengths of the G-wire appears to be due to the difference in surface properties because these affect the formation of DNA nanostructures. Although the length of the G-wire as measured using TEM is longer than that as measured using AFM, the images suggest that the G-wire is a long and relatively rigid nanowire.

The AFM measurements also confirmed the reversible switch in G-wire formation. Figure 5c shows a typical AFM image of G1 in the presence of Ni^{2+} and Na_2EDTA . A significant image was not observed, indicating that, in the absence of Ni^{2+} , G1 does not fold into a high-order structure in the presence of Ni^{2+} and Na_2EDTA . Therefore, it can be concluded that Ni^{2+} induces a structural transition in G1 from an antiparallel G-quadruplex to a G-wire and that Na_2EDTA induces the reverse structural transition from a G-wire to an antiparallel G-quadruplex. These results are the first direct demonstration of G-wire formation that can be switched and controlled using Ni^{2+} and Na_2EDTA .

We also studied the morphology of G1 in the presence of Co^{2+} or Zn^{2+} using AFM. High-order structures were observed in the presence of these metal ions, but the morphologies of the high-order structures in the presence of Co^{2+} (Supporting Information Figure S7a) and Zn^{2+} (Supporting Information Figure S7b) were different from those in the presence of Ni^{2+} (Figure 5b). Specifically, in the presence of Co^{2+} or Zn^{2+} , the structures were globular, whereas in the presence of Ni^{2+} , the

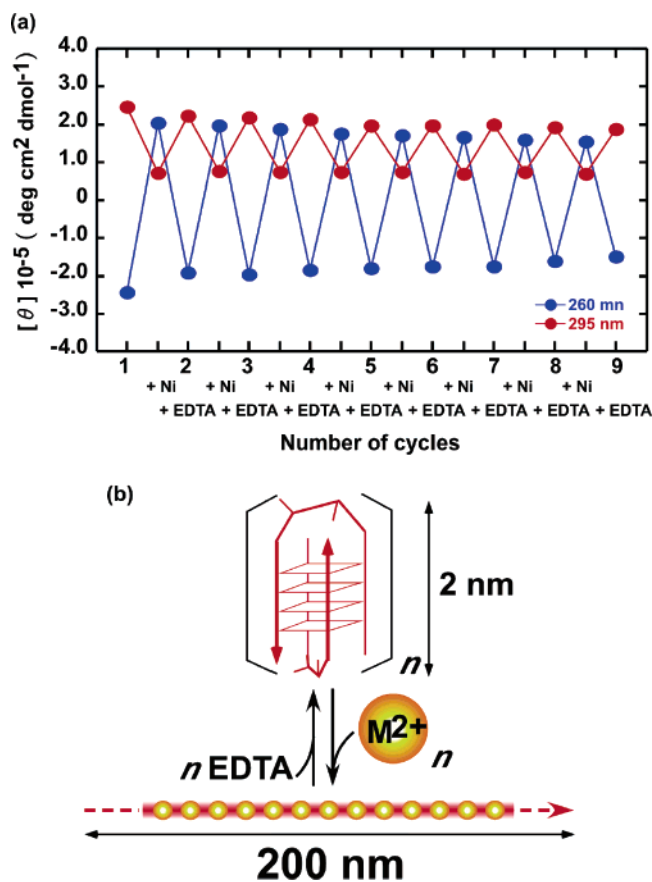


Figure 6. (a) Cycling of the switch as observed by measurement of the CD intensity at 295 nm (red) and 260 nm (blue) at 4 °C. The first cycle was produced by addition of 100 μM NiCl_2 followed by addition of 120 μM Na_2EDTA . The second and later cycles were produced by alternating addition of 100 μM NiCl_2 and 100 μM Na_2EDTA . (b) Schematic illustration of the structural switch of G1 triggered by metal ions. Red squares and yellow circles indicate G-quartets (four-guanine plane) and metal ions, respectively. Rods in the loop region in the top illustration indicate the bipy units.

structure was linear. These results indicate that Ni^{2+} is more effective at inducing G-wire formation by G1 than Co^{2+} or Zn^{2+} , which is consistent with the CD and native PAGE results. Although further investigations of the G-wire structure in the presence of different metal ions are required, the difference in the AFM images implies that the morphology of the high-order structures of G1 can be controlled by divalent metal ion species.

Multiple Cycling of the Structural Switch. The reversibility of the G-wire switch was further investigated by examining the effect of alternating addition of Ni^{2+} and Na_2EDTA . Figure 6a shows the CD intensity of 5 μM G1 at 260 and at 295 nm during repeated addition of Ni^{2+} and Na_2EDTA . In the first cycle, the antiparallel G-quadruplex to G-wire transition was induced by adding 100 μM Ni^{2+} and the reverse transition was induced by adding 120 μM Na_2EDTA . The second and later cycles were induced by alternating addition of 100 μM Ni^{2+} and 100 μM Na_2EDTA . Each cycle led to the generation of 100 μM Ni^{2+} –EDTA complex as a waste product. Direct binding of excess divalent metal ions to G-quadruplexes could lead to irreversible aggregation of G-wires, which would cause difficulties in demonstrating multiple cycling of the switch;^{7a} however, the conditions used here favor formation of Ni^{2+} –EDTA complexes so that waste product accumulation does not hamper the process

for at least 8 cycles. The average cycling efficiency (η) was estimated using the following equation:²¹ $\eta = (F_n/F_0)^{1/n}$, where n is the number of cycles and F_n and F_0 are the CD intensity changes during the n th and initial cycles, respectively. The η values of the switch estimated from the CD intensity changes at both 260 and 295 nm were 0.95, indicating only 5% loss per cycle. This high cycling efficiency suggests that irreversible aggregation of G1 was not induced by divalent metal ion binding to the bipy unit. These results indicate that a G-wire switch can be developed by incorporating bipy units, which allows precise control of G-wire formation by addition of a divalent metal ion and its chelating agent (Figure 6b).

Since the kinetics of the structural transition between the antiparallel G-quadruplex and the G-wire are also important for practical usage, we further investigated the time course of the structural transition of 5 μM G1 at 4 °C by monitoring the CD intensity change at 260 nm (Supporting Information Figure S8a). We found that the transition was very slow. The structural transition from the antiparallel G-quadruplex to the G-wire induced by 100 μM Ni^{2+} at 4 °C took 50 h (Supporting Information Figure S8b). Only half of the structural transition from the G-wire to the antiparallel G-quadruplex induced by 120 μM Na_2EDTA took two weeks (data not shown). These speeds are too slow for many applications. However, the transition from the antiparallel G-quadruplex to the G-wire at 25 °C took only 2 h (Supporting Information Figure S8b), indicating that a higher reaction temperature can accelerate the transition. Moreover, Mergny et al. reported that the speed of G-quadruplex formation is drastically accelerated by having a longer stretch of guanine.²³ Therefore, further acceleration of the structural transition is also possible.

Significance of the G-wire Switch. Switchable molecular machines based on the structural conversion of DNA by metal ions, protons, and fuel DNA strands have been described.^{24,25} For example, Alberti and Mergny used DNA duplex–quadruplex exchange as the basis of a nanomolecular machine²⁴ and Liu and co-workers constructed a DNA nanomachine based on pH-dependent i-motif formation.^{25b,c} Furthermore, Dittmer et al. developed a switchable DNA aptamer device regulated by fuel DNA strands.^{25d} These studies used nanoscale movements in DNA molecules as the basis for functional and dynamic devices. The supramolecular G-wire switch developed here has some advantages as a functional nanodevice over these smaller DNA devices. For example, in our G-wire, the bipy unit is directly adjacent to each G-quadruplex unit, and because the DNA molecule has numerous bipy units, binding of divalent metal ions leads to the generation of a divalent metal ion array. There are only a few examples of one-dimensional metal ion arrays based on DNA templates,²⁶ and the array developed here is much longer than those used in these previous studies. These

(23) Mergny, J.-L.; Cian, A. D.; Ghelab, C.; Saccà, B.; Lacroix, L. *Nucleic Acids Res.* **2005**, *33*, 81–94.

(24) Alberti, P.; Mergny, J.-L. *Proc. Natl. Acad. Sci. U.S.A.* **2003**, *100*, 1569–1573.

(25) (a) Simmel, F. C.; Dittmer, W. U. *Small* **2005**, *1*, 284–299. (b) Liu, D.; Balasubramanian, S. *Angew. Chem., Int. Ed.* **2003**, *42*, 5734–5736. (c) Liu, D.; Bruckbauer, A.; Abell, C.; Balasubramanian, S.; Kang, D.-J.; Klenerman, D.; Zhou, D. *J. Am. Chem. Soc.* **2006**, *128*, 2067–2071. (d) Dittmer, W. U.; Reuter, A.; Simmel, F. C. *Angew. Chem., Int. Ed.* **2004**, *116*, 3634–3637.

(26) (a) Tanaka, K.; Tengeji, A.; Kato, T.; Toyama, N.; Shionoya, M. *Science* **2003**, *299*, 1212–1213. (b) Zimmermann, N.; Meggers, E.; Schultz, P. G. *Bioorg. Chem.* **2004**, *32*, 13–25. (c) Clever, G. H.; Polborn, K.; Carell, T. *Angew. Chem., Int. Ed.* **2005**, *44*, 7204–7208.

divalent metal ions also make it possible to address the G-wire structure by utilizing specific complex formation between divalent metal ions and functional molecules.

In the present study we chose G1, which can form an intermolecular antiparallel G-quadruplex, but shorter and longer guanine stretches in the guanine-rich sequences composing the bipy unit(s) should have different responses to the metal ions, given that we previously found that the polymorphic nature of G-quadruplexes was dependent on their sequence, length, and surrounding environment.^{7,27} Thus, combination of the bipy unit and structural polymorphism of the G-quadruplex is potentially useful for the development of various functional and dynamic DNA devices.

Conclusion

The G-wire switch in this study has two important properties that make it useful for the development of DNA-based functional nanomaterials. First, incorporation of bipy units into G-quadruplexes allowed the design and synthesis of a self-assembled G-wire switch that can be controlled by external stimuli, namely, divalent metal ions and a chelating agent. Second, when the G-wire switch developed here binds divalent metal ions, it creates a one-dimensional array of divalent metal ions that is much longer than those previously reported. We have previously reported that telomere DNAs behave as molecular logic gates that respond to chemical input signals.²⁷ These and our current results indicate that it should be possible to produce artificial and natural telomere DNAs that can be regulated by the surrounding conditions for use as novel functional nanobiomaterials that are switchable, controllable, and addressable.

Experimental Section

Materials. We synthesized the oligonucleotide G1 using a normal solid-phase synthetic procedure except that coupling of the phosphoramidite of the bipy unit was carried out for 30 min to ensure that the phosphoramidite would react with the 5'-terminal alcohol of the oligodeoxynucleotide. Synthesis of the phosphoramidite of the bipy unit was reported by Wiederholt and McLaughlin.¹⁰ After deprotection and purification using a C18 column, the purity of the DNA was confirmed to be ~95%. A sample of the purified DNA was analyzed by MALDI-TOF mass spectrometry. G1 was used without purification by reversed-phase high-performance liquid chromatography (HPLC) because HPLC purification leads to contamination with metal ions (mainly Fe ions) that bind tightly to the bipy unit. G2 used in this study was HPLC grade and was purchased from Hokkaido System Science (Sapporo, Japan).

Single-strand concentrations of the DNA oligonucleotides were determined by measuring the absorbance at 260 nm at a high temperature using a Shimadzu 1700 spectrophotometer (Shimadzu, Kyoto, Japan) connected to a thermoprogrammer. The single-strand extinction coefficient of G2 was calculated from mononucleotide and dinucleotide data using a nearest-neighbor approximation.²⁸ The single-strand extinction coefficient of G1 at 260 nm was calculated as follows: $2\epsilon_{(dGGGG)} (41800) + \epsilon_{(bipy\ unit)} (5900)$, resulting in $\epsilon_{(G1)} = 89500$.

(27) Miyoshi, D.; Inoue, M.; Sugimoto, N. *Angew. Chem., Int. Ed.* **2006**, *45*, 7716–7719.

(28) Nakano, S.; Kanzaki, T.; Sugimoto, N. *J. Am. Chem. Soc.* **2004**, *126*, 1088–1095.

CD Measurements. CD experiments utilizing a JASCO J-820 spectropolarimeter (JASCO, Hachioji, Japan) were measured at 4 °C in a 1 cm path length cuvette for 5 μ M total strand concentration of DNA in buffers containing 100 mM NaCl and 50 mM MES (pH 6.0) at 4 °C. The CD spectra were obtained by taking the average of at least three scans made from 200 to 350 nm. The temperature of the cell holder was regulated using a JASCO PTC-348 temperature controller, and the cuvette-holding chamber was flushed with a constant stream of dry N₂ gas to avoid condensation of water on the cuvette exterior. Except for the kinetic analysis, before the measurement, the sample was heated to 90 °C, gently cooled at a rate of 2 °C min⁻¹, and incubated at 4 °C for 30 min.

Gel Electrophoresis. Native gel electrophoresis was carried out on 10% nondenaturing polyacrylamide gels in buffers containing 100 mM NaCl and 50 mM MES (pH 6.0) in the presence and absence of 50 μ M divalent metal ions at 4 °C. Ice-cold loading buffer (5 μ L of 40% glycerol and 1% blue dextran) was mixed with 5 μ L of 5 μ M DNA sample. Gels were stained with GelStar nucleic acid gel stain (Cambrex, ME) and imaged using FLS-5100 film (Fuji Photo Film Co. Ltd., Tokyo, Japan). Before the measurement, the sample was heated to 90 °C, gently cooled at a rate of 2 °C min⁻¹, and incubated at 4 °C for 30 min.

UV–Vis Measurements. UV–vis spectra utilizing a Shimadzu 1700 spectrophotometer (Shimadzu, Kyoto, Japan) equipped with a temperature controller were measured in a 1 cm path length cuvette for 20 μ M total strand concentration of DNA in buffers containing 100 mM NaCl and 50 mM MES (pH 6.0) in the presence and absence of various concentrations of NiCl₂ at 4 °C. The cuvette-holding chamber was flushed with a constant stream of dry N₂ gas to avoid condensation of water on the cuvette exterior. Before the measurement, the sample was heated to 90 °C, gently cooled at a rate of 2 °C min⁻¹, and incubated at 4 °C for 30 min.

Atomic Force Microscopy. G1 (100 μ M) was dissolved in buffers containing 100 mM NaCl, 50 mM MES (pH 6.0), and 50 μ M NiCl₂. The DNA sample was heated to 90 °C for 10 min, gently cooled at a rate of 1.0 °C min⁻¹, and incubated at 4 °C for 3 days. These samples were diluted 500-fold in distilled water, adjusted to 2 mM MgCl₂, and 10 μ L was deposited onto a freshly cleaved mica substrate, which was then washed in distilled water for ~1 min and dried under a stream of N₂ gas. The DNA samples were imaged by tapping-mode AFM on a Digital Instruments Nanoscope IIIa (Veeco, Santa Barbara, CA) with MPP tips. Image analysis was performed using Nanoscope software after removing the background slope by flattening images. Height and length of the DNA samples were analyzed using the Nanoscope software.

Acknowledgment. We thank Drs. Kensuke Akamatsu and Hidemi Nawafune of Konan University for their assistance with the TEM study and Yumi Ueda for collecting CD spectra and the PAGE data. H.K. received a Research Fellowship from the Japan Society for the Promotion of Science for Young Scientists. This study was supported in part by Grants-in-Aid and the “Academic Frontier” Project (2004–2009) from MEXT, Japan.

Supporting Information Available: Procedures for synthesizing the phosphoramidite of the bipy unit and Figures S1–S8. This material is available free of charge via the Internet at <http://pubs.acs.org>.

JA068707U